Solid-to-Solid Phase Transformations in Inorganic Materials 2005
Volume 2: Displacive Transformations • Fundamentals of Phase Transformations • Experimental Approaches to the Study of Phase Transformations • Computer Approaches to Simulation of Phase Transformations • Phase Transformations in Novel Systems or Special Materials
Edited by James M. Howe, David E. Laughlin, Jong K. Lee, Ulrich Dahmen, and William A. Soffa
TMS (The Minerals, Metals & Materials Society), 2005

TEMPORAL EVOLUTION OF SUB-NANOMETER COMPOSITIONAL PROFILES ACROSS THE γ/γ' INTERFACE IN A MODEL Ni-Al-Cr SUPERALLOY

Chantal K. Sudbrack[1], Ronald D. Noebe[2], and David N. Seidman[1]

[1]Department of Materials Science and Engineering, Northwestern University,
2220 Campus Drive, Evanston, IL 60208-3108 USA
[2]NASA John H. Glenn Research Center; 21000 Brookpark Rd.; Cleveland, OH 44135 USA

Keywords: interface composition; diffusion-limited growth; nanostructure; nickel alloys;

Abstract

Early-stage phase separation in a Ni-5.2 Al-14.2 Cr at.% superalloy, isothermally decomposing at 873 K, is investigated with atom-probe tomography. Sub-nanometer scale compositional profiles across the γ/γ'($L1_2$) interfaces demonstrate that both the γ-matrix and the γ'-precipitate compositions evolve with time. Observed chemical gradients of Al depletion and Cr enrichment adjacent to the γ'-precipitates are transient, consistent with well-established model predictions for diffusion-limited growth, and mark the first detailed observation of this phenomenon. Furthermore, it is shown that Cr atoms are kinetically trapped in the growing precipitates.

Introduction

The seminal work of Schmuck et al. [1] and Pareige et al. [2] combined atom-probe tomography (APT) and lattice kinetic Monte Carlo (LKMC) simulations to analyze in 3D the earliest stages of solid-solid phase separation, that is, the genesis, microstructural evolution and compositional development of nanometer-sized precipitates. Images obtained with APT are direct space 3D atom-maps (post-mortem), where atoms are positioned with sub-nanometer spatial resolution. To address the earliest stages of phase separation with APT sophisticated computer based analytical methods are needed. One such method, the proximity histogram compositional profile [3], developed at Northwestern University, generates a 1D radial compositional profile, from 3D data, that originates from a defined isoconcentration surface(s) (which is independent of the surface topology and feature size), and has been effective in addressing quantitatively interfacial segregation at nanometer-sized precipitates [4,5]. Our research combines APT and LKMC simulations to investigate early-stage phase separation in a nondilute Ni-Al-Cr model superalloy. At 873 K, the Ni-5.2 Al-14.2 Cr at. % solid-solution, γ, contains a low-to-moderate supersaturation of Al and Cr. When aged (0.17–1024 h), $L1_2$-ordered $Ni_3(Al_xCr_{1-x})$ precipitates form via a first-order phase transformation, producing a high number density ($N_v \sim 10^{24}$ m^{-3}) of spheroidal nanometer-sized γ'-precipitates. This article scrutinizes the compositional profiles associated with these γ/γ' interfaces, obtained by the analysis of APT images with the proximity histogram method [3], as a function of aging time.

Experimental

High purity constituent elements were induction melted under an Ar atmosphere to minimize oxidation, and then chill cast to produce master ingots. Inductively coupled plasma atomic-emission spectroscopy measured an average alloy composition of 80.5 Ni-5.2 Al-14.2 Cr at. %.

The cast ingot was homogenized at 1573 K for 24 hours yielding coarse (0.5–2 mm diam.), equiaxed, and twinned grains. The temperature was then decreased to 1123 K and the ingot was annealed for 3 h in the γ-phase field. After water quenching, homogenized sections were aged at 873 K for times ranging from 120 s to 1024 h, quenched, cut, and then electropolished to produce sharp needle-shaped specimens for APT experiments. APT data collection was performed at a specimen temperature of 40.0 ± 0.3 K, a pulse fraction (pulse voltage/steady state dc voltage) of 19%, a pulse frequency of 1.5 kHz (conventional APT) or 200 kHz (*LEAP*® tomograph), and a gauge pressure of < 6.7 x 10^{-8} Pa. Analysis alignment near the 001-crystallographic pole permits the resolution of {001} planes in the APT analysis direction, as seen in Figure 1c. Further experimental and analytical details are found in [6,7].

Results and Discussion

Figure 1 displays a small subset (15 x 15 x 30 nm^3) from an APT image of a specimen aged for 4 h. Omitting the Ni atoms for clarity, the 3D atom distributions of Al (in red) and Cr (in blue) atoms within this volume (Figure 1a) establish clear visual evidence of phase separation of Al-rich γ̃′precipitates and Cr-rich γ-matrix. In this alloy, where the equilibrium phase partitioning of solute is not particularly strong at 873 K, it is useful to omit the atoms within the image and to visualize the precipitation with isoconcentration surfaces (particularly when the mean radius, <*R*>, is less than 1 nm), by delineating the γ/γ′ interfaces with a mid-point concentration threshold, 9 at. % Al for this alloy, Figure 1b. The morphology of the γ′-precipitates is a mixture of individual spheroidal precipitates and interconnected precipitates in various stages of coagulation and coalescence (Figure 1b), as detected by APT for t = 0.25–256 h, and discussed in detail elsewhere [6,7]. For this alloy, the 9 at. % Al isoconcentration surface renderings resolve γ′-precipitates with R as small as 0.45 nm (20 *detected* atoms). The value of N_v for γ′-precipitates is determined directly by counting, while the individual values of R for γ′-precipitates are measured with volume-equivalent R values for the best-fit-ellipsoid about the atoms within single precipitates (Figure 1c). Along the APT analysis direction, the $L1_2$ Al-rich {002} planes are clearly resolved, as can be seen in Figure 1c for 4 h, where the Al and Cr atoms in the γ̃′precipitates are displayed.

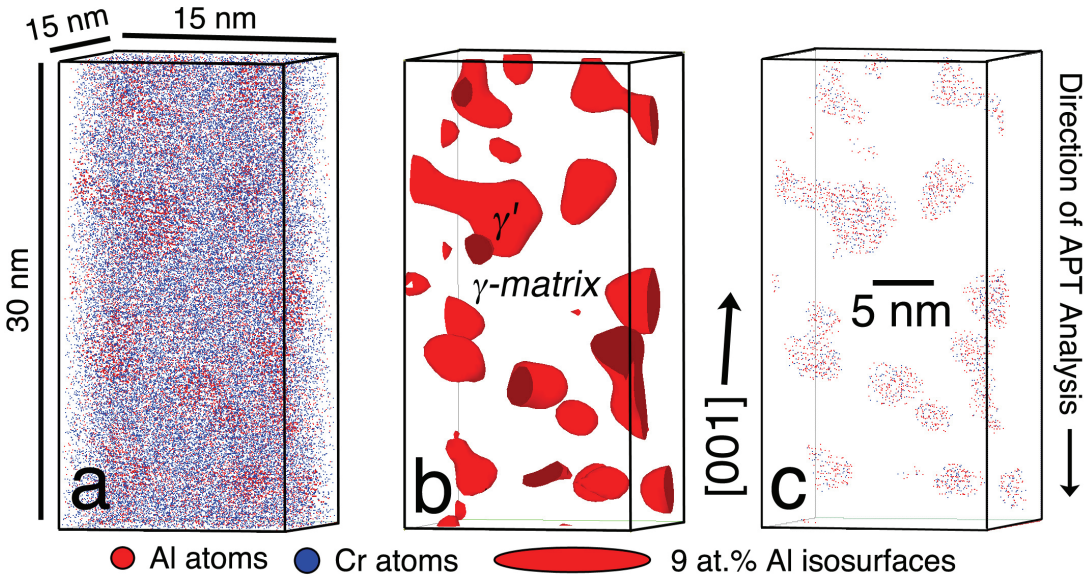

Figure 1. A 15 x 15 x 30 nm^3 subset of an APT analysis performed near [001]-direction of a Ni-5.2 Al-14.2 Cr at.% specimen aged for 4 h at 873 K displaying: (a) Al and Cr atoms; (b) the γ′-precipitates delineated by red 9 at.% Al isoconcentration surfaces; (c) Al and Cr atoms within the $L1_2$-ordered γ′-precipitates, where Al-rich {002} planes are clearly resolved.

Figure 2 presents the full nanostructural evolution of the γ′-precipitation process at 873 K for aging times up to 1024 h within a series of APT images, 10 x 10 x 25 nm^3 subsets each containing 125,000 atoms, while Table I contains their measured <*R*> and N_v values. Compositional measurements obtained with the proximity histogram method average over all isoconcentration surfaces within the analyzed volume; the values obtained are statistically more significant when averaged over many precipitates. The high N_v values for the time scale investigated allows many precipitates to be analyzed for each aging time (Table I), for example, at peak N_v, (3.2 ± 0.6) x 10^{24} m^{-3} after 4 h of aging, 173.5 precipitates are analyzed (Table I), producing smooth sub-nanometer compositional profiles (Figure 3). The <*R*> values change by a full order of magnitude, where <*R*> = 0.74 ± 0.24 nm when the γ′-phase is first detected after 0.166 h of aging and <*R*> = 7.7 ± 3.3 nm for 1024 h. Based on the measurements in Table I, three decomposition regimes are identified: (i) nucleation (*t* = 0.166–0.25 h); (ii) concomitant nucleation and growth (*t* = 0.25–4 h); and (iii) concomitant growth and coarsening (*t* ≥ 4 h).

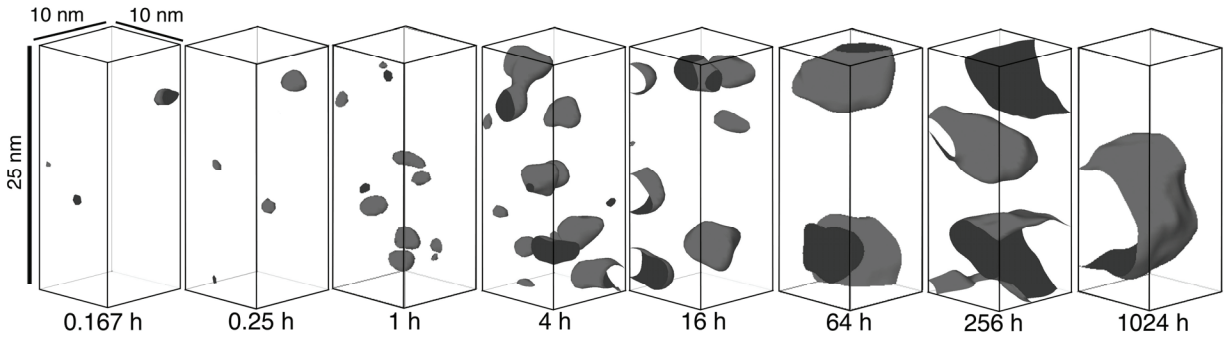

Figure 2. Temporal evolution of the γ′-nanostructure in Ni-5.2 Al-14.2 Cr at.% specimens aged at 873 K is revealed within a series of APT images. Each parallelepiped is a 10 x 10 x 25 nm^3 subset of the analyzed volume and contains approximately 125,000 atoms. The γ/γ′ interfaces are delineated in gray with 9 at.% Al isoconcentration surfaces and individual atoms are not exhibited for the sake of clarity.

TABLE I. Measured Mean Radius (<*R*>) and Number Density (N_v) of the γ′-Precipitates as a Function of Aging Time at 873 K [6,7]

Aging time (h)	Number of γ′-precipitates analyzed[a]	<*R*> ± σ (nm)	N_v ± σ (x 10^{24} m^{-3})
0.167	7.5	0.74 ± 0.24	0.36 ± 0.13
0.25	74	0.75 ± 0.14	2.1 ± 0.4
1	100	0.89 ± 0.14	2.5 ± 0.5
4	173.5	1.27 ± 0.21	3.2 ± 0.6
16	101	2.1 ± 0.4	1.49 ± 0.27
64	46	2.8 ± 0.6	0.49 ± 0.17
256	81[b]	4.1 ± 0.8	0.24 ± 0.04
1024	6	7.7 ± 3.3	0.11 ± 0.06

[a.] The number of precipitates analyzed is smaller than the total number of precipitates intersected during APT analyses as single precipitates intersected partially by the sample volume contribute 0.5 to this quantity.

[b.] For the 256 h aging state, analyses of 11 and 70 precipitates by the conventional APT and the *LEAP*® tomograph, respectively, were performed.

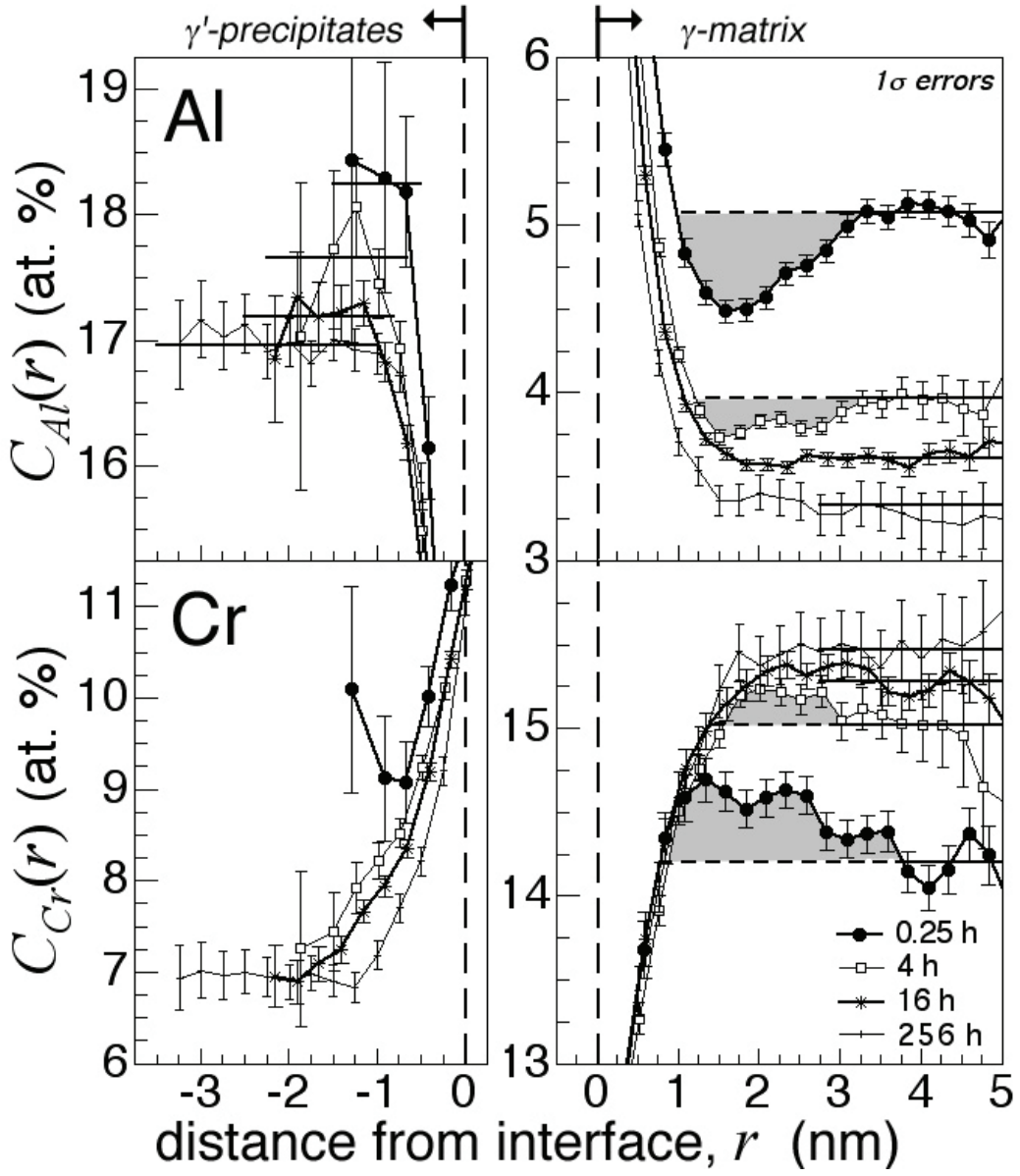

Figure 3. Concentration profiles of Ni-5.2 Al-14.2 Cr at.% aged at 873 K for different aging times are averaged across the γ/γ'-interface for tens to hundreds of γ'-precipitates (TABLE I), which were generated using the proximity histogram method [3]. The shaded regions emphasize an enrichment of Cr or a depletion of Al into the matrix, adjacent to the γ/γ'-interfaces, that are transient. Solid lines denote the plateau concentrations in the precipitates' core (*left*) and in the matrix far-field (*right*).

Concentration profiles generated by the proximity histogram method are presented in Figure 3 for only four of the aging times investigated for the sake of clarity. The compositions of both the γ and γ′-phases continually evolve. With increasing aging time, the far-field concentrations (solid-lines on the *right-side* of Figure 3) of Al in the matrix decrease, while the Cr far-field concentrations increase, characteristic of decreasing supersaturations as Al partitions to γ′-precipitates and Cr to the γ-matrix. In 1949 Zener [8] solved the quasi-stationary (quasi-steady-state) diffusion problem for a spherical precipitate undergoing diffusion-limited growth and obtained a solution that appears in many standard materials science textbooks. Additionally, in 1958 Ham solved the general time-dependent problem for a regular array of growing spherical precipitate [9], which includes higher order transient terms in the general solution for the concentration as a function of both position and time. Ham's solution shows that the transients decay exponentially with increasing aging time until the growth is dominated by a single term. Experimentally, as shown on the *right-side* of Figure 3, we observe a depletion of Al and an enrichment in Cr adjacent to the interface into the matrix, which for the 0.25 h aging state extends nearly 3 nm from the γ/γ′ interface. Furthermore, the degree of depletion (or enrichment) is transient, and disappears completely after 16 h of aging, where the change in solute supersaturation with time after 16 h, in the matrix, is small ($d\Delta C/dt \rightarrow 0$), implying that the system is in a quasi-stationary-state but not a stationary state. Our observations mark the first experimental verification of the time-dependent nature of the concentration profile(s) predicted by Ham's general theory of diffusion-limited growth.

Contrary to what is commonly assumed in many classical models for nucleation, growth or coarsening, the precipitate composition in this alloy evolves significantly with increasing time as shown in Figure 3. The Al concentration, even at the shortest aging times, is constant throughout the precipitate cores (solid-lines on the *left-side* of Figure 3) and decreases continuously from a constant 19.1 ± 2.8 at.% at t = 0.17 h to 16.70 ± 0.29 at.% at 1024 h. Detailed thermodynamic analyses [6] demonstrate that this observed Al enhancement results from capillarity. The γ′-precipitates also exhibit an enhanced solubility of Cr that decays with time, which is contrary to the thermodynamic predictions by CALPHAD models [6]. Until 64 h of aging, a gradual gradient in Cr concentration across the interface through the core region is present. To ascertain the gradient's origin, the diffusivity (D_{Cr}) of Cr in the γ′-precipitate is estimated from data at 256 h, where the Cr profile is flat. The root-mean-squared diffusion distance is taken as twice the average γ′-precipitate diameter, 8.2 ± 1.6 nm. Employing $D_{Cr} = \sqrt{\langle x^2 \rangle}^{\,2} / 6t$, the diffusivity of Cr in the γ′-phase containing 7 to 10 at.% Cr is (4.9 ± 1.9) x 10^{-23} m^2 s^{-1} at 873 K, which is 2 to 5 times greater than the measured tracer diffusivity of Cr in pure Ni_3Al, 1.4 x 10^{-23} m^2 s^{-1} [11]. Since atomic diffusion is concentration dependent, this estimate is reasonable. Hence, during the formation of a stable nucleus, Cr atoms are kinetically trapped within the small growing γ′-precipitates, until a local equilibrium can be established after 64 h.

Summary

For a Ni-5.2 Al-14.2 Cr at.% superalloy aged isothermally at 873 K, the time dependent concentration profiles across the precipitate/matrix interface (Figure 3), obtained by the proximity histogram method [3], reveal: (i) both the γ-matrix and γ′-precipitate compositions evolve temporally; (ii) the presence of transient chemical gradients in the matrix adjacent to the interface, consistent with the general time-dependent theory of diffusion-limited growth [9]; and, (iii) a gradual gradient in Cr from the interface into the precipitate core that persists to 64 h due to Cr entrapment during precipitate nucleation and growth.

Acknowledgements

This research was sponsored by the National Science Foundation, grant DMR-0241928. C. K. Sudbrack received partial support from an NSF graduate research fellowship. We also would like to extend our gratitude to Dr. T. F. Kelly for use of an Imago Scientific Instruments *LEAP*® tomograph for some of the results obtained.

References

1. C. Schmuck, P. Caron, A. Hauet, and D. Blavette, "Ordering and Precipitation of Gamma' Phase in a Low Supersaturated Ni-Cr-Al Model Alloy: An Atomic Scale Investigation," *Philos Mag A*, 76 (1997), 527-542.

2. C. Pareige, F. Soisson, G. Martin, and D. Blavette, "Ordering and Phase Separation in Ni-Cr-Al: Monte Carlo Simulations vs. Three-Dimensional Atom Probe," *Acta Mater*, 47 (1999), 1889-1899.

3. O. C. Hellman, J. A. Vandenbroucke, J. Rüsing, D. Isheim, and D. N. Seidman, "Analysis of Three-Dimensional Atom-Probe Data by the Proximity Histogram," *Micros Microanal*, 6 (2000), 437-444.

4. D. Isheim and D. N. Seidman, "Subnanometer-Scale Chemistry and Structure of α–Iron/Molybdenum Nitride Heterophase Interfaces," *Mater Metall Trans A*, 33 (2002), 2317-2326.

5. E. A. Marquis, D. N. Seidman, M. Asta. C. Woodward, and V. Ozolins, "Mg Segregation at Al/Al_3Sc Heterophase Interfaces on an Atomic Scale: Experiments and Computations," *Phys Rev Let*, 91 (2003), 036101: 1-4.

6. C. K. Sudbrack, "Decomposition Behavior in Model Ni-Al-Cr-X Superalloys: Temporal Evolution and Compositional Pathways on a Nanoscale" (Ph.D. thesis, Northwestern University, 2004). http://arc.nucapt.northwestern.edu/refbase/show.php?record=16

7. K. E. Yoon, "Temporal evolution of the chemistry and nanostructure of multicomponent model Ni-based superalloys" (Ph.D. thesis, Northwestern University, 2004). http://arc.nucapt.northwestern.edu/refbase/show.php?record=15

8. C. Zener, "Theory of growth of spherical precipitates from solid solution," *J Appl Phys*, 20 (1949) 950-953.

9. F. S. Ham, "Theory of diffusion-limited precipitation," *Phys Chem Solids*, 6 (1958), 335-351.

10. Y. Minamino, S. B. Jung, T. Yamane, and K. Hirao, "Diffusion of cobalt, chromium, and titanium in Ni_3Al," *Metall Trans A*, 23 (1992), 2783-2790.